Stereoselective Catalysis of a Retro-Michael Reaction by Class Mu Glutathione Transferases. Consequences for the Internal Distribution of Products in the Active Site

Jihong Chen and Richard N. Armstrong*

Department of Chemistry and Biochemistry, University of Maryland, College Park, Maryland 20742

Received December 16, 1994[⊗]

The reaction of glutathione (GSH) with *trans*-4-phenyl-3-buten-2-one (PBO) is readily reversible in aqueous solution with an apparent (pH-dependent) equilibrium constant at pH 8 of 6.4×10^2 M^{-1}. Two class mu isoenzymes of GSH transferase from rat (M1-1 and M2-2) and two site specific mutants (M1-1/V9I and M2-2/I9V) catalyze the addition of GSH to PBO and the elimination of GSH from the two diastereomeric products (isomers A and B) of 4-(*S*-glutathionyl)-4-phenyl-2-butanone with varying degrees of efficiency and stereoselectivity, with the major kinetic product in the addition reaction (isomer A) being the preferred substrate for the elimination reaction. The kinetic stereoselectivity of the addition reaction and the steady-state kinetics of the elimination reactions with product isomers A and B are used to estimate internal stereochemical equilibrium constants in which product isomer B is predominant. This result is consistent with the internal equilibrium constants measured under conditions of enzyme in excess. The results can be used to construct reaction coordinate diagrams for the interconversion of central complexes in the enzyme-catalyzed reactions. The possible metabolic consequences of the reversibility of additions of GSH to α,β-unsaturated carbonyl compounds are discussed.

Introduction

The glutathione *S*-transferases catalyze a variety of reactions involving the addition of glutathione (GSH)[1] to electrophilic substrates. A number of these reactions represent key steps in the detoxication of endogenous and xenobiotic alkylating agents that are essentially irreversible (e.g., epoxide ring openings). An exception is the conjugate addition of GSH to Michael-acceptor substrates, which, because of the acidic nature of the carbon α to the carbonyl group, is facile in the reverse direction as well. Inasmuch as the Haldane relationship requires that an enzyme catalyze a reaction in both directions, it seems likely that GSH conjugates of α,β-unsaturated carbonyl compounds would be reasonable substrates for the GSH transferases in the reverse (retro-Michael) direction. There are a number of examples of the conjugate addition of GSH to endogenous α,β-unsaturated carbonyl compounds such as 4-hydroxyalkenals and base propenals (*1*–*3*) and xenobiotic substrates such as acrolein (*4*), quinones of polycyclic aromatic hydrocarbons (*5*), and ethacrynic acid (*6*) that may be physiologically relevant to the detoxication of this class of electrophile. Furthermore, it has been recognized for some time that reversible reactions of GSH with electrophiles is an important facet of electrophile transport and toxicity (*7*, *8*). Therefore, it is somewhat surprising that so little attention has been paid to the ability of the enzyme to catalyze the reverse reactions.

The *trans*-4-phenyl-3-buten-2-ones are excellent models for the study of conjugate additions of GSH (*9*). The class mu GSH transferases catalyze the addition of GSH to 4-phenyl-3-buten-2-one (PBO) with good efficiency and in some cases a high degree of stereoselectivity (*10*). For example, the rat M2-2 isoenzyme[2] produces about 90% of one diastereomeric product (Scheme 1) while isoenzyme M1-1 exhibits very little stereoselectivity, giving roughly equal amounts of the two possible products (*10*, *13*, *14*). It has been proposed that the stereoselective behavior of the class mu isoenzymes is dependent, in part, on the identity of the side chain at position 9, which is valine in M1-1 and isoleucine in M2-2 (*14*, *15*). Although the forward enzyme-catalyzed reactions have been well characterized with this and related substrates, there is no information on the ability of the enzyme to catalyze the reverse reaction. In addition, the position of the chemical equilibrium for this reaction has not been established.

In this paper we report a kinetic determination of the equilibrium constant for the addition of GSH to PBO in aqueous solution and that the class mu GSH transferases catalyze the stereoselective decomposition of the two diastereomeric Michael adducts with efficiencies that are competitive with the forward reactions. The kinetics of the forward and reverse reactions are used to estimate an internal equilibrium distribution of products in the active site that is opposite that of the kinetic product distribution. The position of the internal stereochemical equilibrium is shown to be in satisfactory agreement with the kinetic results.

Materials and Methods

General Materials and Methods. Glutathione, *trans*-4-phenyl-3-buten-2-one, buffer salts, solvents, and all other

* Address correspondence to this author. Phone: (301) 405-1812; FAX: (301) 405-7956; email: ra19@umail.umd.edu.

⊗ Abstract published in *Advance ACS Abstracts,* April 15, 1995.

[1] Abbreviations: GSH, glutathione; PBO, *trans*-4-phenyl-3-buten-2-one; CD, circular dichroism; EDTA, ethylenediaminetetraacetic acid; DSS, 2,2-dimethyl-2-silapentane-5-sulfonate; Tris, tris(hydroxymethyl)-aminomethane.

[2] The nomenclature for the rat isoenzymes follows that recommended by Mannervik et al. (*11*) for the human isoenzymes. Although the rat isoenzymes were not specifically named, it is clear in this nomenclature that the class mu isoenzyme 3-3 from rat corresponds to M1-1 while isoenzyme 4–4 should be designated M2-2 (*12*).

0893-228x/95/2708-0580$09.00/0

Scheme 1

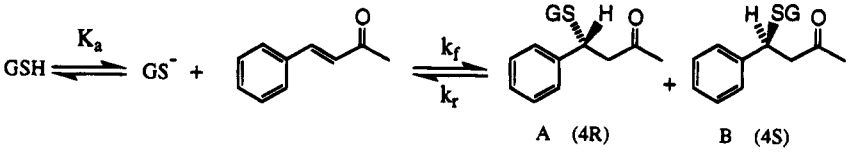

chemical reagents were of the highest quality commercially available. Oligonucleotides for site-specific mutagenesis were purchased from Midland Certified Reagent Co. (Midland, TX). Sequenase Version 2 DNA sequencing kit was purchased from U.S. Biochemical Corp. In general, all duplex DNA fragments derived from the digestion of plasmids were purified by gel electrophoresis and recovered from the gel using the Geneclean methodology (Bio 101 Inc., La Jolla, CA). Expression vectors were produced using *Escherichia coli* strain MM294CI+ that had been transformed with the appropriate plasmids or ligation products. Mutant expression plasmids were purified by the Qiagen column method (Qiagen Inc., Chatsworth, CA) and sequenced to assure the absence of any unwanted mutations.

Construction of Mutant Expression Vectors and Preparation of Enzymes. The construction of the expression vector designated pGT33MXV9I encoding the V9I mutant of the M1-1 isoenzyme was reported by Shan and Armstrong (*15*). The expression plasmid pGT44MXI9V encoding the I9V mutant of isoenzyme M2-2 was prepared in a similar way by cassette mutagenesis. The 30-base pair cassette which encodes residues 1−9 and lies between the unique *Nde*I and *Sac*II restriction sites of pGT44 (14) was replaced by a synthetic linker harboring the appropriate mutation.

The recombinant plasmids, harvested from cultures of MM294CI+, were introduced into the temperature sensitive *E. coli* strain M5219 for efficient expression of the enzymes. Briefly, cultures of bacteria harboring the desired plasmids were grown in a 1 L fermenter as previously described (16). The cells were harvested by centrifugation, and the supernatant was applied to an *S*-hexylglutathione affinity column. The enzyme from the affinity column was passed through a hydroxylapatite column, and the active fractions were concentrated and dialyzed against 10 mM potassium phosphate (pH 7.0) containing 1 mM EDTA and 1 mM dithiothreitol. Protein concentrations were determined using an $E^{0.1\%}_{280} = 1.69$.

Synthesis and Characterization of Product Diastereomers. The two diastereomeric addition products were prepared by specific-base-catalyzed addition of GSH to PBO. A solution of 1.5 mmol of GSH in 2.5 mL of H_2O was placed in a 25 mL round-bottom flask and purged with N_2. The reaction was initiated by adding 0.75 mL of 6 N NaOH followed by 1 mmol of PBO dissolved in 2.5 mL of CH_3CN. The reaction mixture was stirred under N_2 at room temperature for 16 h. The solution was then adjusted to pH 4.5 with acetic acid and extracted four times with 10 mL of ethyl acetate. The product isomers, designated A and B in order of their elution on reversed-phase HPLC, were separated and purified using a (10 mm × 250 mm) Beckman Ultrasphere C8 column eluted with 26% CH_3OH in H_2O containing 0.1% CF_3CO_2H. Fractions containing each isomer were lyophilized, and their purity was confirmed by analytical HPLC. The two products were characterized by ^{1}H-NMR spectroscopy using a Bruker AM-400 spectrometer. ^{1}H-NMR (400 MHz, D_2O, ref) DSS *Isomer A*: δ 1.96 (s, 3H, phenylbutanone CH_3), δ 1.96 (m, 2H, ^3J = 7.1 Hz, γ-Glu β-CH_2), δ 2.27 (t, 2H, ^3J = 7.1 Hz, γ-Glu γ-CH_2), δ 2.58 (dd, 1H, ^2J = 14.2 Hz, ^3J = 7.9 Hz, Cys β-CH_2), δ 2.76 (dd, 1H, ^2J = 14.5 Hz, ^3J = 5.4 Hz, Cys β-CH_2), δ 3.01 (d, 2H, ^3J = 7.4 Hz, phenylbutanone CH_2), δ 3.77 (s, 2H, Gly CH_2), δ 3.77 (m, 1H, γ-Glu α-CH), δ 4.08 (m, 1H, ^3J = 7.7 Hz, ^3J = 5.2 Hz, Cys α-CH), δ 4.17 (t, 1H, ^3J = 7.5 Hz, phenylbutanone CH), δ 7.20 (m, 5H, phenylbutanone C_6H_5); *Isomer B*: δ 1.95 (s, 3H, phenylbutanone CH_3), δ 2.02 (m, 2H, ^3J = 7.1 Hz, ^3J = 6.7 Hz, γ-Glu β-CH_2), δ 2.33 (m, 2H, ^3J = 7.4 Hz, γ-Glu γ-CH_2), δ 2.47 (dd, 1H, ^2J = 14.2 Hz, ^3J = 8.5 Hz, Cys β-CH_2), δ 2.63 (dd, 1H, ^2J = 14.1 Hz, ^3J = 5.3 Hz, Cys β-CH_2), δ 2.97 (dd, 1H, ^2J = 17.4 Hz, ^3J = 7.6 Hz, phenylbutanone CH_2), δ 3.01 (dd, 1H, ^2J = 17.6 Hz, ^3J = 7.3 Hz, phenylbutanone CH_2), δ 3.73 (s, 2H, Gly CH_2), δ 3.85 (m, 1H, ^3J = 6.5 Hz, γ-Glu α-CH), δ 4.13 (t, 1H, ^3J = 7.5 Hz, phenylbutanone CH), δ 4.21 (m, 1H, ^3J = 8.4 Hz, ^3J = 5.3 Hz, Cys α-CH), δ 7.20 (m, 5H, phenylbutanone C_6H_5). The CD spectra were obtained on a JASCO J-700 spectropolarimeter.

Chemical Equilibrium between GSH and PBO. The apparent equilibrium constant for the reaction of GSH and PBO was determined at 25 °C and pH 8 from the dependence of the first-order rate constant for the approach to equilibrium on the concentration of GSH under pseudo-first-order conditions. Reactions of 20 μM PBO and 2−10 mM GSH in 0.1 M Tris buffer (pH 8.0) were followed for at least 10 half-lives at 290 nm. The data were fitted to a single exponential to determine k_{obs}.

Enzyme Kinetics. The method for assay of the enzyme has been described previously (*9*, *14*). The enzymatic reactions of GSH with PBO were carried out at 25 °C in 0.1 M potassium phosphate and 1 mM EDTA (pH 6.5) in the presence of saturating (2 mM) GSH as the fixed substrate and PBO as the varied substrate (20−100 μM) with an enzyme concentration of between 0.1 and 0.2 μM. The reaction was followed at 290 nm ($\Delta\epsilon$ = −17 000 M^{-1} cm^{-1}). The elimination reactions with isomers A and B were followed at the same wavelength ($\Delta\epsilon$ = 17 000 M^{-1} cm^{-1}) under the same temperature and buffer conditions in the absence of GSH and PBO. The enzyme and substrate concentrations differed depending on the isoenzyme or mutant used. For the more efficient M2-2 isoenzyme and the I9V mutant the active site concentration was 0.04 −0.1 μM with a substrate concentration range of 5−100 μM. The M1-1 and V9I concentrations were between 2 and 7 μM with a substrate concentration range of 20−200 μM.

Kinetic and Internal Equilibrium Product Distributions. The kinetic stereoselectivities of the various enzymes were determined at short (5−15 min) reaction times at pH 6.5 with catalytic amounts (ca. 2−10 μM enzyme) in the presence of saturating (1 mM) GSH and 600 μM PBO essentially as previously described (*10*, *14*). The internal equilibrium distribution of products were determined under conditions of enzyme in excess. Enzyme (1 mM active sites) was incubated with 200 μM GSH and 200 μM PBO for 15−3 h. The reactions were quenched by the addition of 0.5 M ammonium acetate (pH 3.8) and analyzed by reversed-phase HPLC. The final distribution of products was constant with incubation times from 15 min to 3 h.

Results

Preparation and Characterization of Product Diastereomers. The conjugate addition products of the reaction of GSH with PBO were easily prepared in basic solution and separated by reversed-phase HPLC. Although the best separation of the two diastereomers was obtained using 0.1 M ammonium acetate buffer (pH 3.8) containing 12.5% CH_3OH (10), removal of the buffer by lyophilization resulted in decomposition and epimerization of the conjugates. Epimerization was avoided by using a less basic solvent system of 0.1% CF_3CO_2H containing 26% CH_3OH. The ^{1}H-NMR spectra of the products were fully consistent with their structures. The circular dichroism spectra for the two diastereomers, shown in Figure 1, are nearly the same but opposite in sign as expected for the chromophores epimeric at C4. The spectra are not mirror images of one another due to

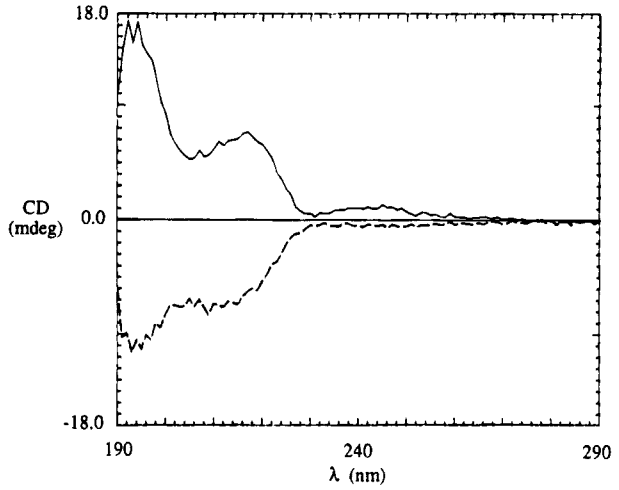

Figure 1. Circular dichroism spectra of product isomers A (top trace, —) and B (bottom trace, - - -) at pH 3.8 and 25 °C. Concentrations of isomers A and B are 27 and 20 μM, respectively.

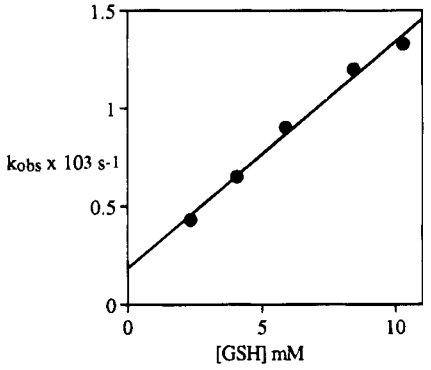

Figure 2. Dependence of k_{obs} for the approach to equilibrium on the concentration of GSH at pH 8 and 25 °C. The solid line is a linear regression fit of the data to the equation $k_{obs} = k_f$ [GSH] + k_r, where $k_f = 0.116 \pm 0.01$ M^{-1} s^{-1} and $k_r = (1.8 \pm 0.2) \times 10^{-4}$ s^{-1}.

the contribution of the peptide, particularly below 220 nm. The absolute configurations of isomers A and B are not known and should not be inferred from Scheme 1. The isomers were stable to epimerization in the lyophilized state and for several hours at room temperature in the buffers used for enzymatic reactions.

Chemical Equilibrium for the Reaction of GSH with PBO. The position of the apparent chemical equilibrium for reaction of GSH_{aq} with PBO at pH 8 was derived from the dependence of the observed rate constant for the approach to equilibrium on the concentration of GSH, as shown in Figure 2 where $k_{obs} = k_f$[GSH] + k_r. The rate constants for the forward ($k_f = 0.116 \pm 0.01$ M^{-1} s^{-1}) and reverse [$k_r = (1.8 \pm 0.2) \times 10^{-4}$ s^{-1}] reactions were obtained from the slope and intercept of the plot, respectively. The apparent (pH-dependent) equilibrium constant at pH 8 is calculated from $K_{app} = k_f/k_r = 6.4 \times 10^2$ M^{-1}. The actual reactive species is the thiolate, GS^-_{aq}, so that the equilibrium constant, K, for the thiolate is obtained from $K = K_{app}(1 + [H]/K_a) = 9.1 \times 10^3$ M^{-1}, where $K_a = 7.59 \times 10^{-10}$ (the acid dissociation constant of GSH, $pK_a = 9.12$) and [H] is the hydronium ion concentration. It is clear that the chemical equilibrium between PBO and GS^-_{aq} favors product and that the reaction is readily reversible ($k_r = 1.8 \times 10^{-4}$ s^{-1}). Even though the transition states leading to the two products are diastereomeric and therefore not necessarily isoenergetic, there is no observable stereoselectivity in the chemical reaction.

Kinetics of Enzyme-Catalyzed Retro-Michael Reactions. The glutathione transferases, the M2-2 isoenzyme in particular, catalyze the stereoselective formation of product by differential stabilization of the two possible diastereomeric transition states (*10*). Therefore, the enzyme is expected to catalyze the stereoselective elimination of GSH from product isomers A and B, as well, in which the preferred substrate for the elimination is the major product of forward reaction. Consistent with this expectation is the observation that the enzyme, even the highly stereoselective M2-2 isoenzyme, accelerates the approach to chemical equilibrium, eventually giving approximately equal amounts of A and B. In addition, a catalytic amount of any of the enzymes discussed here catalyzes the decomposition of isomer A to an equilibrium mixture of approximately equal amounts of both A and B. For example, incubation of 1 μM M1-1 (the least efficient enzyme) with 100 μM isomer A at pH 6.5 gives an equilibrium mixture within 48 h at 25 °C. Isomer A alone under the same conditions exhibits only 3% epimerization.

The class mu isoenzymes catalyze the elimination of GSH from both diastereomeric conjugates of PBO with varying degrees of efficiency and stereoselectivity as indicated by the data in Table 1. The M2-2 isoenzyme which exhibits a high efficiency and stereoselectivity in the conjugate addition (forward) reaction (*10*) is also quite efficient in the reverse reaction. Isomer A, the major kinetic product in the forward direction, is the preferred substrate for the elimination reaction catalyzed by M2-2. A comparison of the turnover number for isomer A with the first-order rate constant (k_r) for the spontaneous decomposition in aqueous solution indicates that the enzyme accelerates the reverse reaction by a factor of $>10^3$. The stereoselectivity of M2-2 in the elimination is quite pronounced in that $(k_{cat}/K_m^A)_r$ exceeds $(k_{cat}/K_m^B)_r$ by a factor of more than 400 while the ratio $(k_{cat}^A)_r/(k_{cat}^B)_r$ is almost 100.[3] In contrast, M1-1, which is much less efficient and has little or no ability to discriminate between the prochiral faces of PBO in the forward reaction, exhibits only a slight preference for isomer A [$(k_{cat}/K_m^A)_r/(k_{cat}/K_m^B)_r = 5.5$ and $(k_{cat}^A)_r/(k_{cat}^B)_r = 3.6$] in the reverse direction.

Previous work with mutants of the M1-1 isoenzyme has suggested that the side chain at position 9 influences the kinetic stereoselectivity of the addition of GSH to PBO (*14*, *15*). The influence of the Val/Ile mutation on the stereoselectivity of the reverse reaction was tested by interchange of the side chains at this position with the M1-1/V9I and M2-2/I9V mutants as indicated in Table 1. The V9I mutation in M1-1 increases the efficiency of the enzyme toward isomer A but has no effect on the reaction of isomer B. Although several types of comparisons of the kinetic properties of native and mutant enzymes can be made, perhaps the most informative is in the ability of enzyme to discriminate between isomer A and B as reflected in the ratio $(k_{cat}/K_m^A)_r/(k_{cat}/K_m^B)_r$. This ratio increases from 5.5 to 37 with M1-1/V9I and decreases from 426 to 58 with M2-2/I9V. Qualitatively, this is the expected result based on the kinetic stereoselectivity of these enzymes in the forward direction.

[3] The subscripts r and f are used to designate catalytic rate constants for the reverse and forward reactions, respectively. The superscripts A and B designate the product or substrate isomer.

Table 1. Kinetic Constants and Kinetic Stereoselectivity for the Addition and Elimination of GSH to 4-Phenyl-3-buten-2-one and from Product Isomers A and B at pH 6.5

substrate	enzyme	k_{cat} (s^{-1})	k_{cat}/K_m ($M^{-1}\,s^{-1}$)	stereoselectivity[a] (mol fraction of A)
PBO	M1-1	0.70 ± 0.01	(3.9 ± 0.1) × 10^3	0.50 ± 0.03
	M1-1/V9I	0.74 ± 0.03	(4.6 ± 0.1) × 10^3	0.89 ± 0.01
	M2-2[b]	8.5 ± 0.7	(4.7 ± 0.2) × 10^4	0.92 ± 0.02
	M2-2/I9V	2.7 ± 0.2	(2.6 ± 0.1) × 10^4	0.85 ± 0.01
isomer A	M1-1	0.0035 ± 0.0001	(1.6 ± 0.1) × 10^2	
	M1-1/V9I	0.014 ± 0.005	(1.4 ± 0.1) × 10^3	
	M2-2	0.61 ± 0.01	(2.9 ± 0.2) × 10^5	
	M2-2/I9V	0.38 ± 0.01	(1.1 ± 0.1) × 10^5	
isomer B	M1-1	0.0011 ± 0.00003	(2.9 ± 0.1) × 10^1	
	M1-1/V9I	0.0010 ± 0.00003	(3.8 ± 0.4) × 10^1	
	M2-2	0.0063 ± 0.0008	(6.8 ± 0.3) × 10^2	
	M2-2/I9V	0.013 ± 0.001	(1.9 ± 0.1) × 10^3	

[a] The kinetic stereoselectivity at short reaction times before the reverse reaction becomes significant. [b] Data from ref 10.

Scheme 2

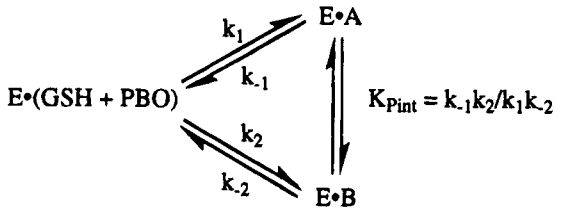

Table 2. Calculated and Observed Internal Stereochemical Equilibrium Constants

enzyme	K_{Pint} (calc)[a]	% E•A (calc)	K_{Pint} (obsd)[b]	% E•A (obsd)
M1-1	2.9–4.6	18–26	2.7	27 ± 1
M1-1/V9I	1.4–2.2	31–42	1.5	40 ± 1
M2-2	4.6–15	6–18	4.6	19 ± 1
M2-2/I9V	3.7–6.5	13–21	2.3	30 ± 1

[a] Calculated using the k_{cat} and kinetic stereoselectivity values from Table 1 and the relationship in eq 1. The range of values is derived from propagation of the errors in the measurements of k_{cat} and the mol fraction of isomer A. [b] Derived from K_{Pint} = [E•B]/[E•A] under conditions of enzyme in excess.

Internal Stereochemical Equilibrium. The internal substrate:product equilibria for the two diastereomers is illustrated in Scheme 2, where k_1, k_{-1}, etc., are the microscopic rate constants for the interconversion of the three central complexes and K_{Pint} is the apparent internal stereochemical equilibrium constant for the two product complexes E•A and E•B defined in the following equation 1:

$$K_{Pint} = [E\cdot B]/[E\cdot A] = k_{-1}k_2/k_1k_{-2} \quad (1)$$

The microscopic rate constants can be estimated from the turnover numbers at steady state given in Table 1. Values for the microscopic rate constants in the forward direction are approximated by the product of the observed k_{cat} for the overall reaction and the mol fraction of the particular stereoisomer formed (e.g., $k_1 \approx (k_{cat}^{A})_f = k_{cat}^{PBO}$ × mol fraction of A). The microscopic rate constants in the reverse direction are assumed to be equivalent to the k_{cat} values derived from the reverse Michael reactions (e.g., $k_{-1} \approx (k_{cat}^{A})_r$). These values were used to calculate K_{Pint} as given in eq 1. In all cases the calculated K_{Pint} > 1 as shown in Table 2. That is, product isomer B is predicted to predominate in the internal equilibria. This is an interesting result since the kinetically preferred product of the forward reaction is usually isomer A (Table 1).

Inasmuch as the steady-state turnover numbers may differ from the microscopic rate constants in Scheme 2, a second determination of K_{Pint} is desirable. The internal stereochemical equilibrium can also be measured directly under conditions of enzyme in excess where all of the product is bound. Thus, an incubation mixture of enzyme (1 mM active sites) with 200 μM GSH and 200 μM PBO was quenched by lowering the pH, and the ratio of the two products was quantified by HPLC. The observed values of K_{Pint} obtained from the measured product ratios are given in Table 1 and are in reasonable agreement with the values derived from steady-state kinetics.

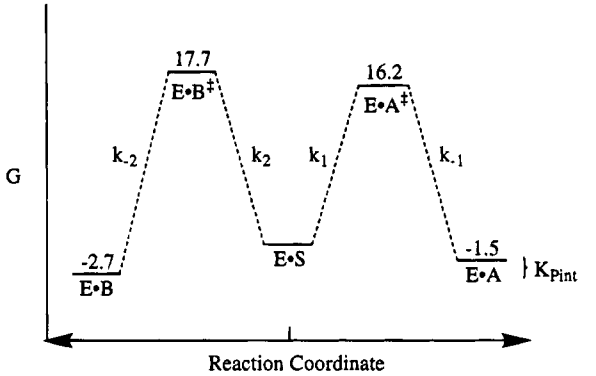

Figure 3. Reaction coordinate diagram for the internal partitioning of enzyme-bound substrates and products for isoenzyme M2-2. For clarity, the two parallel transition states are shown proceeding in opposite directions on the reaction coordinate. The enolic intermediates for the reactions are not considered since it is expected that they are very minor species. The relative Gibbs free energies (kcal/mol) of ground states and transition states are calculated from the turnover numbers for the forward and reverse reactions from the relationship $\Delta G^{\ddagger} = -RT \ln[(k_{cat})h/kT]$, where h is Planck's constant, k is the Boltzmann constant, and T = 298 K. E•S represents the ternary E•(GSH+PBO) complex, which is arbitrarily assigned a free energy of 0.

Discussion

Significance of the Internal Stereochemical Equilibrium. The position of the internal stereochemical equilibrium is a consequence of the microscopic rate constants (Scheme 2) for traversing the barriers between enzyme-bound substrates and enzyme-bound products. That the predominant isomer in the internal equilibrium is the least favored kinetically is best illustrated in the free energy profile of the M2-2 isoenzyme shown in Figure 3. The profile is constructed using the turnover numbers of the forward and reverse reactions to approximate the microscopic rate constants for the internal equilibrium (Scheme 2). It is emphasized that this profile is approximate since the steady-state turnover numbers (k_{cat}) used to construct it may be influenced by external steps (substrate binding and product release) and may

not accurately reflect the microscopic rate constants for the internal chemical steps. Nevertheless, the profile predicts that the E·B product complex is 1.2 kcal/mol more stable than E·A, which is in reasonable agreement with the difference of 0.9 kcal/mol measured directly. The greater stability of E·B suggests that whatever enzymic device that is utilized to stabilize E·A‡ is not manifest in the product (E·A) complex. A similar analysis of the M1-1 isoenzyme predicts a difference of 0.7 kcal/mol between E·B and E·A as compared with the measured value of 0.6 kcal/mol.

Figure 3 also predicts that the product complexes will dominate the internal equilibrium with about 1% or less of the enzyme occupied as the ternary E·(GSH+PBO) complex. It is much more difficult to accurately measure the concentration of the ternary substrate complex. In principle, the fraction of enzyme in the ternary complex can be estimated by measuring the ratio of unreacted substrates (PBO or GSH) to products in a stoichiometric mixture of enzyme, GSH, and PBO at concentrations high enough that all species are enzyme-bound. Analysis of a mixture of 1 mM M2-2 active sites with 1 mM GSH and 1 mM PBO indicates that about 10% of the PBO is unreacted, an amount that is higher than that expected based on the estimates from the turnover numbers. The reason for this difference is unclear. It is possible that under these conditions a significant fraction of PBO is not bound to the enzyme. Nevertheless, it is clear that the ternary E·(GSH+PBO) complex is a minor species in the internal equilibrium.

The observation that one product isomer predominates in the internal equilibrium of the enzyme is of some practical importance since it suggests that it may be possible to obtain single crystals of the enzyme in complex with essentially a single diastereomeric product. If this possibility is realized, then it is a straightforward matter to determine the absolute configurations of the two isomers by X-ray crystallography. However, the value of the structure of the product complex in understanding catalysis may be compromised by the fact that the identity of the predominant product in the internal equilibrium is opposite that of the kinetic product.

Influence of Enzymic Residues on Catalysis. Acceleration of the conjugate addition/elimination reactions by the enzyme may involve the participation of an enzymic electrophile to stabilize the carbonyl oxygen in forming the enolic intermediate and perhaps a base to abstract and deliver the proton at the α-position of the substrate. It has been previously postulated that the hydroxyl group of Tyr115 acts as an electrophilic catalyst in Michael reactions since the Y115F mutants of both M1-1 (17) and M2-2[4] are 50−1000 times less efficient toward PBO than the native enzymes. Since both native enzymes have a tyrosine at position 115, other factors or residues must account for the differences in their efficiencies toward PBO and related substrates. As yet, no side chain has been identified that might act as a base in the removal of the α-proton.

The influence of the side chain at position 9 (Val or Ile) on the kinetic stereoselectivity of the M1-1 isoenzyme is well established (*14*, *15*). As anticipated, the complementary I9V mutation of M2-2 has the complementary effect of decreasing the stereoselectivity of the enzyme, although only slightly. That the V9I and I9V mutations of M1-1 and M2-2 have only a modest influence on the efficiency of the forward and reverse reactions as well as on the position of the internal equilibrium is an indication that this residue fine tunes the observed differences in efficiency and stereoselectivity of M1-1 and M2-2.

Effect of Reversibility on Metabolism. The enzyme-catalyzed elimination of GSH from carbon β to a carbonyl function has potential ramifications for the metabolism and transport of Michael acceptor substrates. For example, the stereochemical outcome of metabolism may very well depend on whether the conjugation reaction has a chance to come to chemical equilibrium. If the initial (kinetic) product(s) is rapidly disposed of either by transport or further metabolism, then it can be expected that the transported GSH conjugate or metabolite (mercapturic acid, for example) will bear the stereochemical imprint of the initial conjugation reaction. In contrast, if the subsequent transport and/or metabolic events occur at rates that are significantly slower than the reverse reaction, then the conjugation reaction will approach chemical (and stereochemical) equilibrium and the kinetic stereoselectivity of the GSH transferase-catalyzed Michael addition would be irrelevant.

The reverse reaction may also be important in the transport and distribution of the electrophilic species within a cell or organism. In fact, the involvement of the reversible nonenzymatic addition of GSH in the transport of toxic electrophiles has been appreciated for some time (*7*, *8*). However, the GSH transferase-catalyzed elimination reactions have not been examined in any detail. It is easily imaginable that, after the initial addition reaction, the conjugate could be transported to another cellular compartment (*18*, *19*) and the electrophile released at a new site by GSH transferase-catalyzed elimination of GSH. The transport could be facilitated intracellularly by the enzyme itself (*18*) or intercellularly through the ATP-dependent glutathione-conjugate export pump (*19*, *20*).

The extent or velocity of the reverse reaction and hence its importance to the metabolic disposition of a compound will depend, in part, on the concentration of GSH. The elimination reaction will be disfavored at high (normal) concentrations of GSH since GSH can effectively compete for the active site of the enzyme. Nevertheless, in cells or compartments that have low concentrations of GSH the influence of the enzyme-catalyzed elimination reaction on metabolism is anticipated to be much greater.

Conclusions. The enzyme-catalyzed elimination of GSH from conjugates of α,β-unsaturated carbonyl compounds provides another avenue to study the catalytic mechanism of the GSH transferases. Moreover, the enzyme-catalyzed reversibility of Michael additions may influence the metabolism and transport of this class of electrophile to an extent that is not generally appreciated.

Acknowledgment. This work was supported by NIH Grant GM 30910.

[4] J. Chen and R. N. Armstrong, unpublished results.

References

(1) Ålin, P., Danielson, U. H., and Mannervik, B. (1985) 4-Hydroxyalk-2-enals are substrates for glutathione transferase. *FEBS Lett.* **179**, 267−270.

(2) Danielson, U. H., Esterbauer, H., and Mannervik, B. (1987) Structure−activity relationships of 4-hydroxyalkenals in the conjugation catalyzed by mammalian glutathione transferases. *Biochem J.* **247**, 707−713.

(3) Berhane, K., Widersten, M., Engström, Å., Kozarich, J. W., and Mannervik, B. (1994) Detoxication of base propenals and other α,β-unsaturated aldehyde products of radical reactions and lipid peroxidation by human glutathione transferases. *Proc. Natl. Acad. Sci. U.S.A.* **91**, 1480–1484.
(4) Beauchamp, R. O., Jr., Andjelkovich, D. A., Kligerman, A. D., Morgan, K. T., and Heck, H. d'A. (1985) A critical review of the literature on acrolein toxicity. *CRC Crit Rev. Toxicol.* **14**, 309–380.
(5) Morgenstern, R., DePierre, J. W., Lind, C., Guthenberg, C., Mannervik, B., and Ernster, L. (1981) Benzo(a)pyrene quinones can be generated by lipid peroxidation and are conjugated with glutathione by glutathione S-transferase B from rat liver. *Biochem. Biophys. Res. Commun.* **99**, 682–690.
(6) Ploemen, J. H. T. M., van Ommen, B., and van Bladeren, P. J. (1990) Inhibition of rat and human glutathione *S*-transferase isoenzymes by ethacrynic acid and its glutathione conjugate. *Biochem. Pharmacol.* **40**, 1631–1635.
(7) Baillie, T. A., and Slatter, J. G. (1991) Glutathione: A vehicle for the transport of chemically reactive metabolites in vivo. *Acc. Chem. Res.* **24**, 264–270.
(8) Monks, T. J., Anders, M. W., Dekant, W., Stevens, J. L., Lau, S. S., and van Bladeren, P. J. (1990) Glutathione conjugate mediated toxicities. *Toxicol. Appl. Pharmacol.* **106**, 1–19.
(9) Habig, W. H., Pabst, M. J., and Jakoby, W. B. (1974) Glutathione *S*-transferases. The first enzymatic step in mercapturic acid formation. *J. Biol. Chem.* **249**, 7130–7139.
(10) Kubo, Y., and Armstrong, R. N. (1989) Observation of a substituent effect on the stereoselectivity of glutathione *S*-transferases toward para-substituted 4-phenyl-3-buten-2-ones. *Chem. Res. Toxicol.* **2**, 144–145.
(11) Mannervik, B., Awasthi, Y. C., Board, P. G., Hayes, J. D., Di Ilio, C., Ketterer, B., Listowsky, I., Morgenstern, R., Muramatsu, M., Pearson, W. R., Pickett, C. B., Sato, K., Widersten, M., and Wolf, C. R. (1992) Nomenclature for human glutathione transferases. *Biochem. J.* **282**, 305–308.
(12) Klinga-Levan, K., Andersson, A., Hanson, C., Ridderström, M., Stenberg, G., Mannervik, B., Vajdy, M., Szpirer, J., Szpirer, C., and Levan, G. (1993) Mapping of glutathione transferase (GST) genes in the rat. *Hereditas* **119**, 285–296.
(13) Zhang, P., and Armstrong, R. N. (1990) Construction, expression and preliminary characterization of chimeric class *mu* glutathione *S*-transferases with altered catalytic properties. *Biopolymers* **29**, 159–169.
(14) Zhang, P., Liu, S., Shan, S., Ji, X., Gilliland, G. L., and Armstrong, R. N. (1992) Modular mutagenesis of exons 1, 2, and 8 of a glutathione *S*-transferase from the *mu* class. Mechanistic and structural consequences for chimeras of isoenzyme 3-3. *Biochemistry* **31**, 10185–10193.
(15) Shan, S., and Armstrong, R. N. (1994) Rational reconstruction of the active site of a class mu glutathione transferase. *J. Biol. Chem.* **269**, 32373–32379.
(16) Zhang, P., Graminski, G. F., and Armstrong, R. N. (1991) Are the histidine residues of glutathione *S*-transferase important in catalysis? An assessment by ^{13}C-NMR spectroscopy and site-specific mutagenesis. *J. Biol. Chem.* **266**, 19475–19479.
(17) Ji, X., Johnson, W. W., Sesay, M., Dickert, L., Prasad, S. M., Ammon, H. L., Armstrong, R. N., and Gilliland, G. L. (1994) Structure and function of the xenobiotic substrate binding site of a glutathione *S*-transferase as revealed by X-ray crystallographic analysis of product complexes with the diastereomers of 9-(*S*-glutathionyl)-10-hydroxy-9,10-dihydrophenanthrene. *Biochemistry* **33**, 1043–1052.
(18) Listowsky, I., Abramovitz, M., Homma, H., and Niitsu, Y. (1988) Intracellular binding and transport of hormones and xenobiotics by glutathione *S*-transferases. *Drug Metab. Rev.* **19**, 305–318.
(19) Ishikawa, T. (1992) The ATP-dependent glutathione S-conjugate export pump. *Trends Biochem. Sci.* **17**, 463–468.
(20) Olive, C., and Board, P. (1994) Glutathione S-transport by cultured human cells. *Biochim. Biophys. Acta* **1224**, 264–268.

TX9401728